Thermoresponsive Shape Memory Characteristics of Polyurethane Electrospun Web

Seung Eun Chung,[1,2] Chung Hee Park,[1,2] Woong-Ryeol Yu,[2,3] Tae Jin Kang[2,3]

[1]*Department of Clothing and Textiles, Seoul National University, Seoul, Korea*
[2]*Intelligent Textile System Research Center, Seoul National University, Seoul, Korea*
[3]*Department of Materials Science and Engineering, Seoul National University, Seoul, Korea*

Received 24 September 2009; accepted 12 August 2010
DOI 10.1002/app.33167
Published online 19 October 2010 in Wiley Online Library (wileyonlinelibrary.com).

ABSTRACT: Electrospun web (ESW) was manufactured and its performance was evaluated to investigate its applicability as an intelligent clothing material using shape memory polymers. Mixtures of various compositions were applied to make the shape memory polyurethane (SMPU) films and the polyurethane with the best shape memory performance was then selected to make the ESWs. The structural and thermal properties, as well as the shape memory behavior were evaluated. The air permeability, the water vapor transmission, and the water resistance were measured. The ESW having a high orientation due to an elongation in the process of the electrospinning showed a higher melting point than the film and its shape recovery was improved. The ESW showed a good moisture and air permeability due to the fact that its structural characteristics incorporate countless nano-sized pores. Because of this, the ESW maintained in its expanded state below the transition temperature showed improved moisture and air permeabilities. Therefore, it can be concluded that the SMPU web proved to have potential for intelligent clothing material.
 J Appl Polym Sci 120: 492–500, 2011

Key words: polyurethanes; membranes; thin films; nanotechnology; high-performance polymers

INTRODUCTION

Shape memory polymers (SMPs) are smart polymers that, as a result of an external stimulus, can change from a temporary deformed shape back to an original shape.[1–4] The shape change is activated most often by a change in the surrounding temperature, but certain materials can also be activated by stress, magnetic fields, electric fields, pH values, UV light, and even water.[5,6] SMPs have many advantages over shape memory alloys, such as easy processing, a low density, a high recovery, a high recoverable strain, and a low manufacturing cost.[7–9]

It has been reported that SMPs have been made of film-shaped thin and poreless membranes. The water vapor permeability of these membranes can undergo a significant increase as temperature increases within a predetermined temperature range. The molecules form a free space in the membrane by micro-Brownian motion above the transition temperature (T_{trans}). Therefore, the application of this membrane to clothing allows heat or moisture to transfer more easily above this T_{trans}, resulting in a better climate control, making the clothing more comfortable.[10–14] Many studies have been done to apply SMPs to the biomedical, electric, and electronic fields, along with industrial materials, but there are few studies applying SMPs, including membrane-shaped shape memory polyurethane (SMPU) films, to clothes. Thus, by applying SMPs to clothing materials, we can expect an improved performance with an improved functionality over that of conventional clothing, by detecting external stimuli that actively protects the human body and improves comfort. Electrospinning is a process capable of producing polymer fibers with nanoscale diameters. The equipment is easy to operate and the membrane can be applied to a wide range of polymer materials. In addition, the ultrafine solid fibers are notable for small diameters, a large surface area to volume ratio, a small pore size, and a high porosity.[15,16] Electrospun web (ESW) shows resistance to microfiller transmission due to the nano-sized pores, so, it shows a good breathability by being able to wick interior sweat. In addition, the outside of the membrane contains a lot of air due to these countless nano-scale pores. There are a variety of advantages, including variable insulative properties.[17] Thus, if we make textiles using this membrane, it is expected to be possible to apply this as a "smart" or intelligent material that has an ultra-lightweight protection function as well as comfort, even under severe conditions. There have been studies regarding the application of SMPs to electrospun

Correspondence to: C. H. Park (junghee@snu.ac.kr).
Contract grant sponsor: National Research Foundation of Korea (NRF); contract grant number: R11-2005-065.

TABLE I
Specification of SMPU

Polymer	PCL M_n (g/mol)	Mole ratio			M_n[a] (g/mol)	M_w[b] (g/mol)	Hard segment content (wt %)
		MDI	PCL	BD			
A	4000	6	1	5	113,000	270,000	33
B	3000	4.5	1	3.5	116,000	288,000	32
C	3000	2	1	1	156,000	396,000	16

[a,b]Average molecular weights were found by gel permeation chromatography.

membranes, along with studies on the evaluation of the shape memory performance of ESWs,[16] but there are few studies on applying SMPs to the membrane of an ESW or to textile materials. The existing shape memory materials are made of films in which a moisture transpiration quality has been added; we think nanoweb membranes will accomplish this transpiration better.

Therefore, an ESW made of SMPs with a good permeation performance, when compared with the existing shape memory films, was manufactured and its performance was evaluated to explore the possibility of its being applied as an intelligent textile material. As the first step, various composite mixtures of SMPU were applied to manufacture films and the resulting characteristics were evaluated. Then, best-performing SMPU was then used to make intelligent ESWs that can change the pore size in accordance with a temperature change. The physical characteristics, the shape memory behavior, the permeation performance, and the screening performance were reviewed. In addition, the permeability and the protection performance changes caused by the shape memory behavior were evaluated by comparing samples with or without shape memory.

EXPERIMENTAL

Materials

The materials were synthesized by Hosung Chemex in one-step process with poly(ε-caprolactone) diol (PCL diol, M_n = 3000 g/mol or 4000 g/mol), 4,4′-diphenylmethane diisocyanate (MDI), and 1,4-butanediol (BD). The ratio between the molecular weight and the reactants of the PCL was changed, resulting in the synthesis of three kinds of polyurethane, as shown in Table I. The chemical structure of PCL-based polyurethane is described in Figure 1.

Preparation of the specimens

To make the reference films, polyurethane chips were melted down and compressed using hot plates. To manufacture the webs, a polyurethane solution of 4–8 wt % was electrospun under 20 ± 3°C, 50 ± 10 RH %, adjusting the voltage between 6 and 16 kV, a feed rate of 1.0–2.5 mL/h, and with a tip-to-collector distance of 5–20 cm. A 1 : 1 mixture of *N*,*N*-dimethylformamide and tetrahydrofuran was used as a solvent. The thicknesses of the films and the ESW were set to 40 μm except in special cases.

Structure and physical properties

To see the structure of the SMPU and the phase separation behavior, an infrared spectrometer (FTIR, Nicolet 6700, Thermo Scientific, USA) was used at the frequency of 32 with a resolution of 8. In addition, the physical properties were determined with an universal testing machine. The tensile test samples had the dimensions of 50 × 10 × 0.5 mm^3. The gauge length and crosshead speed were 20 mm and 10 mm/min, respectively.

Thermal properties

To check out the transition temperatures of the samples in accordance with the change with temperature, a differential scanning calorimetry (DSC Q-1000, TA Instrument, UK) was used with a heating rate of 10°C/min. A dynamic mechanical thermal analysis (DMTA, MARK IV, Rheometric Scientific, UK) was carried out at a heating rate of 5°C/min and a frequency of 1 Hz.

Thermomechanical properties

To evaluate the shape memory behavior, the specimen was drawn by 50% at T_{trans} + 20°C for 5 min, and then, while maintaining the strain, the temperature was cooled to T_{trans} − 20°C. After holding at T_{trans} − 20°C for 5 min, it was unloaded. It was then heated from T_{trans} − 20°C to T_{trans} + 20°C and held for 5 min at T_{trans} + 20°C. The shape retention and shape recovery were obtained based on the following equations.[16]

Figure 1 Chemical structure of the PCL-based polyurethane.

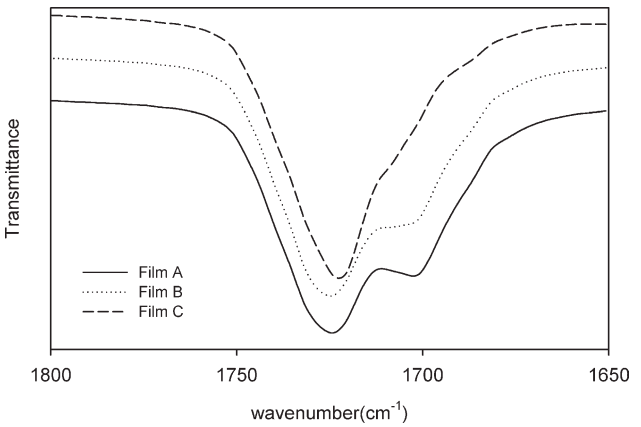

Figure 2 Infrared spectra of the films.

$$\text{Shape retention } (\%) = \varepsilon_f/\varepsilon_m \times 100 \quad (1)$$

$$\text{Shape recovery } (\%) = \{(\varepsilon_m - \varepsilon_r)/\varepsilon_m\} \times 100 \quad (2)$$

where ε_m = strain at the expansion of 50%; ε_f = strain at $T_{trans} - 20°C$; and ε_r = recovery expansion rate at $T_{trans} + 20°C$.

Appearance and pore characteristics

A field emission scanning electron microscope (FE-SEM, SUPRA 55VP, Carl Zeiss, Germany) was used to observe the uniformity of the webs and measure the fiber diameter. The pore size and distribution were measured using a Capillary Flow Porometer (CFP-1500AEL, PMI, USA).

Air and water vapor transmission

The air permeability was measured according to ASTM D 737 and the water vapor transmission (WVT) was measured according to the testing method using calcium chloride per ASTM E 96.

Resistance to water penetration

The resistance to water penetration was determined by the ISO 811 resistance to water penetration–hydrostatic pressure test. A hydrostatic pressure tester (FX3000, Textest, Swiss) was used for this test. The rate of increase of water pressure was set to 60 cm H_2O/min.

RESULTS AND DISCUSSION

Structural characteristics of the films

The structure and phase separation behaviors of the SMPU film were evaluated via FTIR, with the results shown in Figure 2. The two characteristic peaks, around 1705 and 1724 cm^{-1}, are ascribed to the stretching vibration of the carbonyl (—C=O) group in the hard segment. The former peak is due to the presence of hydrogen bonded carbonyl groups formed by phase separation and intermolecular interaction with the —NH in the hard segment, whereas the latter peak is due to the presence of nonhydrogen bonded free carbonyl groups due to dissolving in the matrix of the soft segment. As the hard segment content increases, the peak intensity at 1705 cm^{-1} increased while the peak intensity at 1724 cm^{-1} decreased. A few interactions among the polymeric chains are responsible for the shift of the transmittance peak with the inclusion of more hard segments: (1) the hydrogen bonding between carbonyl group and carbonyl group of the hard segment; (2) the dipole–dipole interaction between the carbonyl groups of the hard segment; and (3) the induced dipole–dipole interaction between the aromatic rings of the hard segment. The hydrogen bonding among the hard segments plus the dipole–dipole interaction between the carbonyl groups will primarily affect the C=O stretching vibration, and the shift of the carbonyl stretch peak suggests that more extensive interactions are being made with an increasing hard segment content.[18–20] Therefore, the phase separation of the PU is gradually well developed with an increasing hard segment content.

By measuring the peak intensity ratio of these two carbonyl groups, it is possible to give an estimate of the degree of the hydrogen bonding. The hydrogen bonding index R is defined as the ratio of the absorption peak A_{1705}/A_{1724}. In association with the change of the NH group absorption peaks, the degree of phase separation (DPS) of the segmented PU can be calculated.[21–23] In addition, the hydrogen bonding index R can be obtained from a baseline approach method:

$$R = C_{bonded}\varepsilon_{bonded}/C_{free}\varepsilon_{free} = A_{1705}/A_{1724} \quad (3)$$

In (3), A is the absorbance, C is the concentration, ε_{bonded} is the extinction coefficient of the peak at 1705 cm^{-1}, and ε_{free} is the extinction coefficient of the peak at 1724 cm^{-1}. The ratio, $\varepsilon_{bonded}/\varepsilon_{free}$, is close to 1.0.[21] DPS can be obtained by using the following equation:

$$DPS = C_{bonded}/(C_{bonded} + C_{free}) = R/R + 1 \quad (4)$$

The calculated DPS values are presented in Table II. For Film A and Film B, which contained the

TABLE II
Degree of Phase Separation for Films

Sample	DPS (%)
Film A	40.1
Film B	38.1
Film C	27.9

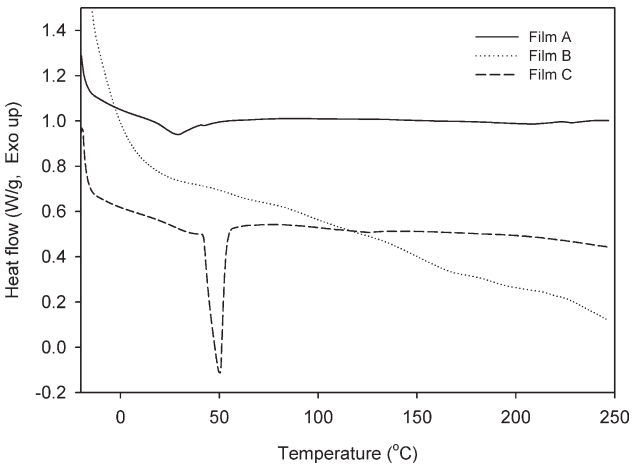

Figure 3 DSC curves of the films measured at a heating rate of 10°C/min.

higher hard segment content than Film C, the phase separation was well developed. The absorption peaks were clearly shown to be around 1705 cm^{-1}.

Thermal properties of the films

To study the thermal behavior of the SMPU materials, a DSC was used with the results shown in Figure 3. Films A and C showed endothermic peaks by soft segment melting at 29°C and 50°C, moreover, Film C showed a very high fusion heat.

The T_{trans} depends on the soft phase/hard phase composition and the molecular weight of the polyol. In previous researches,[24–26] the T_{trans} increases with an increasing soft segment content as well as the molecular weight of the soft segment. In addition, the crystallinity increases with an increase in the soft segment content and molecular weight. For PUs of the same soft segment molecular weight, the crystallinity of the soft segments decreases with an increasing hard segment content. For Film A, because the molecular weight of the PCL was the highest, it was expected to have a high T_{trans}. However, Film A, which had a high hard segment content, showed a bit lower T_{trans} than expected because the crystallization ability of PCL segments is significantly hindered by the connection with the hard segments. Film B had a low PCL molecular weight but it had a higher amount of MDI and BD, which formed a hard segment domain due to the hydrogen bonds and the dipole–dipole interaction.[24,27] Thus, the peak caused by the soft segment did not develop because low PCL molecular weight and high hard segment content had become the critical factors disturbing the crystallization of the soft segment. Film C had the same molecular weight as Film B but contained a higher soft segment content. It is thought that this may act as an advantageous condition for the crystallization development in the soft segment and so increase the T_{trans}.

Figure 4 shows the T_{trans} of the SMPU films via the DMTA measurement. Film A showed a decrease in the modulus around 26°C and showed a transition at 33°C while Film Cs occurred at 54°C. For Film B, the change in the storage modulus at a particular temperature was not observed.

The glassy state and the rubbery state modulus for Film A that had higher soft segment molecular weight were greater than that of Film B. This was because the phase separation and crystallization of the soft segment were well formed. Film C, despite having the same molecular weight in the soft segment as Film B, showed a higher glassy state modulus and lower rubbery state modulus. This was because the crystallization had been well formed due to the higher soft segment content. Film B again showed no determinable T_{trans}.

Shape memory behavior of the films

Figure 5 and Table III exhibit the shape memory behavior of the films. Film C showed the highest values in shape retention, followed by Film A and Film B. The high crystallinity of the soft segment regions and the formation of stable hard segment domains acting as physical crosslinks in the temperature range above the melting temperature of the soft segment crystals are the two necessary conditions for a segmented copolymer with shape memory behavior.[25] When the SMPU has been temporarily transformed, the shape retention is decided by the crystalline structure of the soft segment.[27] The crystallinity of the soft segment also depends on the PCL molecular weight and soft segment content. The crystallinity of soft segments increases with

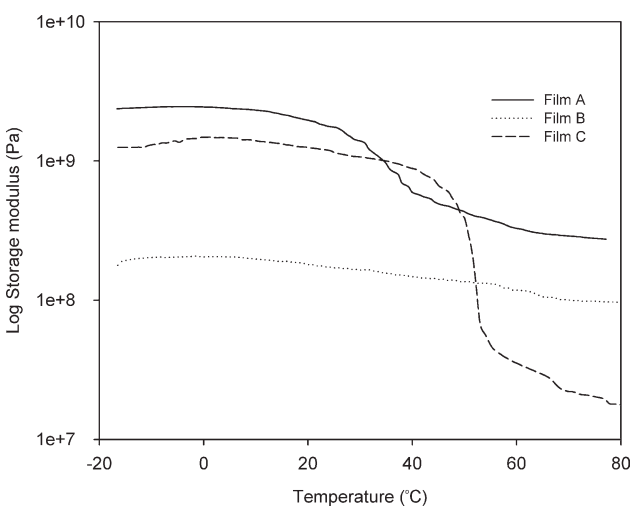

Figure 4 DMTA diagram of the films measured at a heating rate of 5°C/min.

TABLE III
Shape Retention and Recovery of Films

Sample	Shape retention (%)	Shape recovery (%)
Film A	86	85
Film B	68	73
Film C	95	71

increased soft segment content or PCL molecular weight.[26] It seemed that Film C, whose crystallities were well developed due to the high soft segment content, did this well. In the meantime, Film B, which showed the same PCL molecular weight as Film C, but contained a lower soft segment content, had the weakest shape retention. Moreover, Film A, which is similar to Film B in soft segment content, but contained a higher PCL molecular weight than that of Film B, got better shape retention.

With respect to the shape recovery values, Film A showed the best result, followed by Film B and Film C. The shape recovery rate and the recovery speed are mainly related to the stability of the hard segment domains and are dependent on the hard segment content of the copolymers. The insufficient numbers of hard segment domains provides a smaller number of physical crosslinks, which acts similarly to entanglement points.[24–26] As the results of the DPS and DMTA of SMPU film samples, it was observed that Film A was well phase separated to organize soft and hard segments. The rubbery state as well as the glassy state modulus of Film A increased because the phase separation and the soft segment crystallization increased compared with Film B, which was insufficient to organize the soft and hard segments. With the phase separation, hard segment effectively acts like reinforcing fillers for soft segments above the T_m of the soft segment.[24–26] Thus, Film A, which had the greater phase separation, exhibited the best shape recovery. In the meantime, Film B, which showed the similar hard segment content, but contained a low PCL molecular weight, had weak shape recovery compared with Film A. Film C, whose phase separation was not well developed due to the low hard segment content, had the weakest shape recovery.

Therefore, the major issues related to the developments of such PU-based SMPs are the ability to achieve maximum crystallization and stable hard segment domains.[27] For this, it is necessary to properly compose the ratio of the soft segment to the hard segment, while increasing the molecular weight of the soft segment and the hard segment content.

Preparation of the electrospun web

As a result of the evaluation of the performance of the three kinds of SMPU film samples, Film A showed the best results in its physical properties and its shape recovery, along with a satisfactory shape retention. Thus, SMPU A was selected to manufacture the ESW, and uniform fibers were formed from the SMPU solution at concentrations of 4–7 wt %. The optimum electrospinning conditions were determined to be 6.5 kV/1.0 mL/h, 7.5 kV/1.5 mL/h, 9 kV/2.0 mL/h, and 12 kV/2.0 mL/h for the concentrations of 4, 5, 6, and 7 wt %, respectively. Figure 6 shows the FE-SEM images of the electrospun fibers under optimal conditions. The ESW having the finest and most uniform fibers was obtained with a 4 wt % solution. It was found that the diameters of the electrospun fibers increased with an increased concentration of the solution.

Tensile properties of the film and the electrospun web

Figure 7(a) shows the tensile properties of the film and the ESW obtained with 4 wt % solution. The breaking stress of the ESW was similar to that of the film, and the breaking strain of the ESW was higher than that of the film by 30%. In addition, the ESW showed a very low initial modulus value compared with the film because the ESW had a porous structure.

Figure 7(b) shows the breaking stress and strain curves taken from the load per unit weight of the specimens. It was observed that the breaking stress value of the ESW increased by 4.5 times when compared with the film.

Thermal properties of the electrospun web

Figure 8 shows that the DSC curves of the film and the ESW have inflection points at 29°C and 38°C, respectively, corresponding to the T_m of the soft segment. According to Kaursoin and Agrawal,[28] the

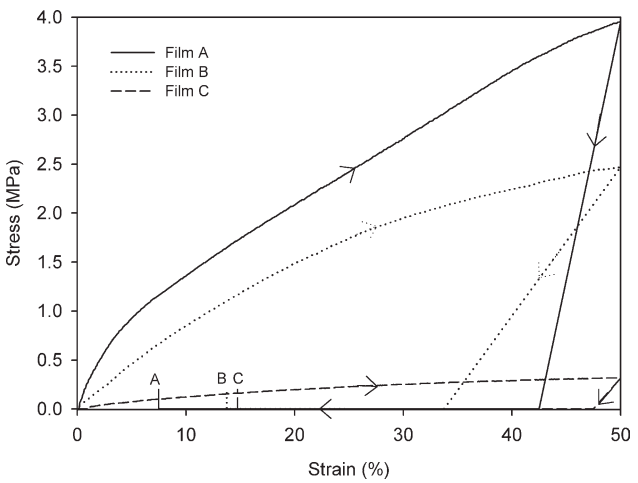

Figure 5 Stress–strain curves for the shape memory behavior of the films, elongated at T_{trans} + 20°C, fixed at T_{trans} − 20°C, and recovered at T_{trans} + 20°C.

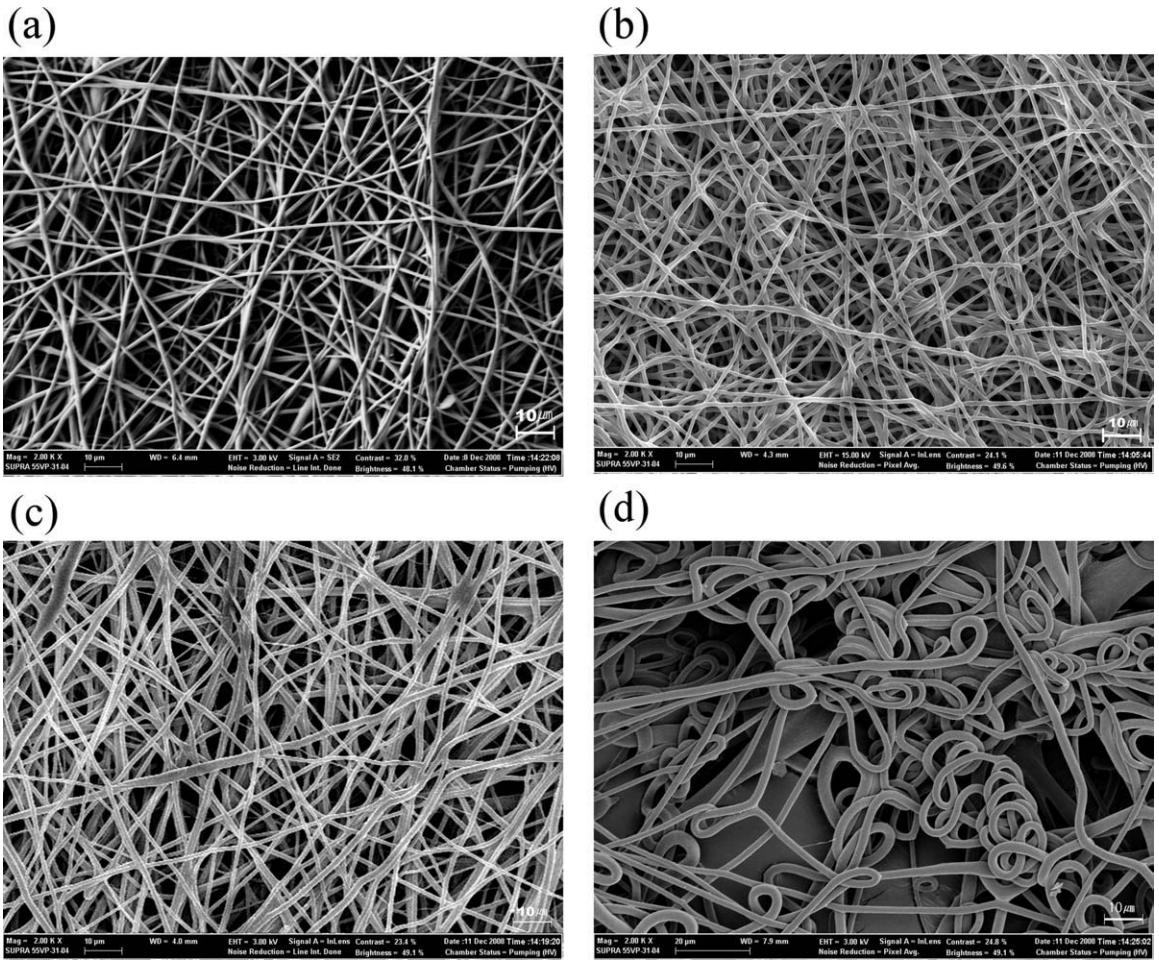

Figure 6 Field emission scanning electron microscopic pictures of the ESW of the various concentration solutions: (a) 4 wt % solution, (b) 5 wt % solution, (c) 6 wt % solution, and (d) 7 wt % solution.

drawing imparts an orientation to the SMP chains and hence improves the shape memory properties due to a stable transformed structure with the hard segment domains strongly bonded with the hydrogen bonds.[28] Thus, the ESW in which an orientation was developed due to an elongation in the process of electrospinning showed a higher melting point than the film.

Shape memory behavior of the electrospun web

From Figure 9(a), the stress value and the shape retention of the ESW showed a lower value than that of the film. It seems that the ESW is structurally weaker than the film as it has a porous structure made of nanofibers.

For the characteristic showing that the ESW is lighter than the film, Figure 9(b) shows the stress–strain curves of the shape memory behaviors expressed by the load per unit weight. It was confirmed that the amount of load per unit weight of the film and the ESW reached a similar level when extended by 50%. The shape recovery of the ESW was improved when compared with the film. As stated earlier, the shape recovery is mainly related to the stability of the hard segment domains.[24–26] Thus, it seems that the shape recovery of the ESW was improved when compared with the film because the electrospun fibers were oriented in the process of electrospinning.

Pore size distribution of the electrospun web

The film and the ESW were manufactured to have 40-μm thicknesses. Figure 10 shows the pore size distributions for the original ESW, the 50% stretched ESW, and the recovered ESW. The pores of the ESW were formed within the range of 144–553 nm, with an average pore size of 346 nm. In addition, the pore sizes of the stretched ESW increased by 1.2–1.5 times when compared with the original ESW. The pore size distribution of the recovered ESW was similar to the original ESW. Of course, in the film, it was impossible to measure the pore size distribution because in film, pores do not exist.

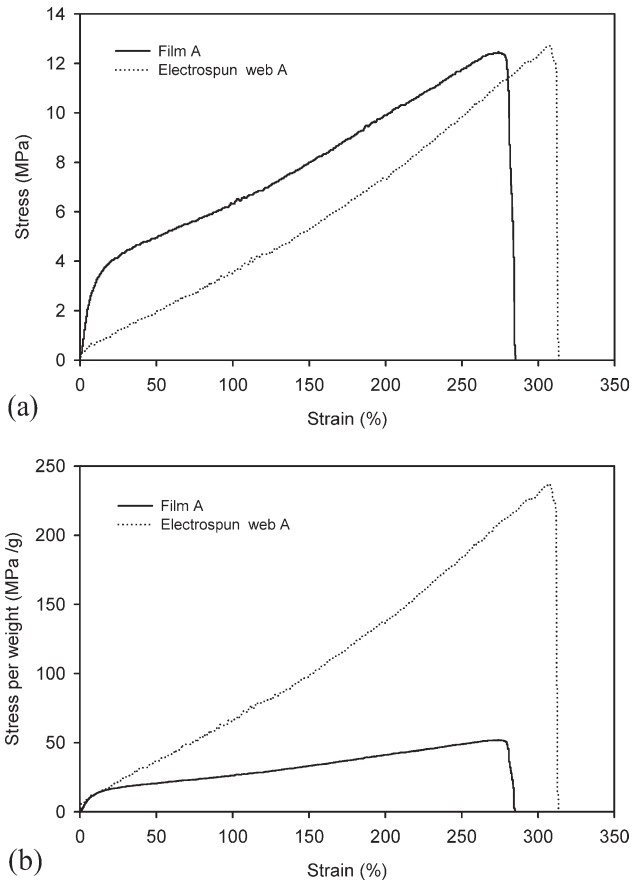

Figure 7 Breaking stress and strain curves of the film and ESW measured at the strain rate of 10 mm/min (thickness: 0.5 mm): (a) the breaking stress–strain curves of the film and ESW, (b) the breaking stress per weight–strain curves of the film and ESW.

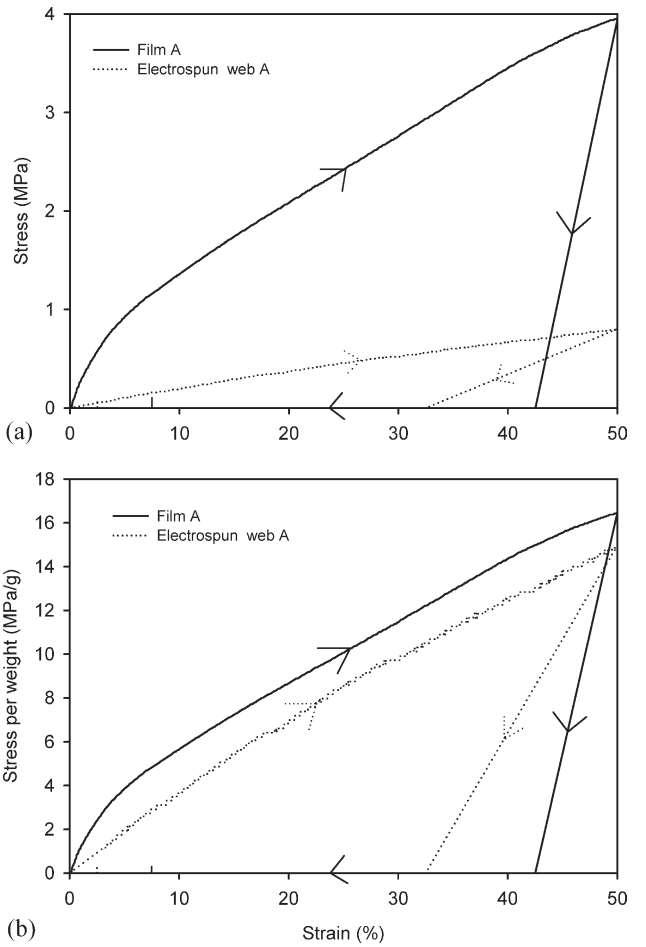

Figure 9 Stress–strain curves for the shape memory behavior of the film and ESW, elongated at T_{trans} + 20°C, fixed at T_{trans} − 20°C, and recovered at T_{trans} + 20°C: (a) the stress–strain curves for the shape memory behavior, (b) the stress per weight–strain curves for the shape memory behavior.

Air and water vapor transmission

Figure 11 shows the air permeabilities of the film and the ESW. It was seen that the ESW showed an air permeability value of 7.0 $cm^3/cm^2/s$ regardless of temperature. The air permeability of the stretched ESW increased 2.5 times at 20°C when compared with the original web. The recovered ESW at 40°C, which had been stretched at 20°C, showed an air permeability similar to that of the original ESW. On the contrary, the film showed little air permeability.

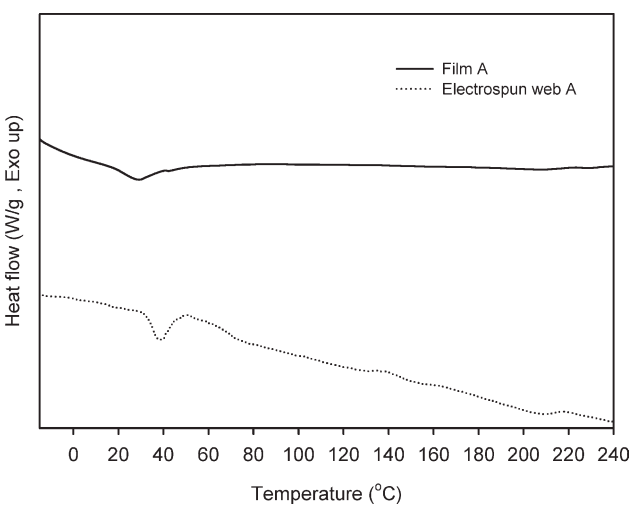

Figure 8 DSC diagram of the film and ESW measured at a heating rate of 10°C/min.

Figure 12 shows the WVT of the film and the ESW. The WVT of the stretched ESW increased below the T_{trans} compared with the original ESW because the stretched ESW maintained extended pores below the T_{trans}. The recovered ESW at 40°C, which had been stretched at 20°C, showed a WVT similar to the original ESW. It was observed that the WVT of the samples increased with temperature as the vapor pressures also increased.

In the meantime, the film had a remarkably low WVT compared with the ESW. The film showed a very low WVT at 20°C, and the WVT of the film increased a little above T_{trans}. It was reported that the change of the WVT in the SMPU film was due

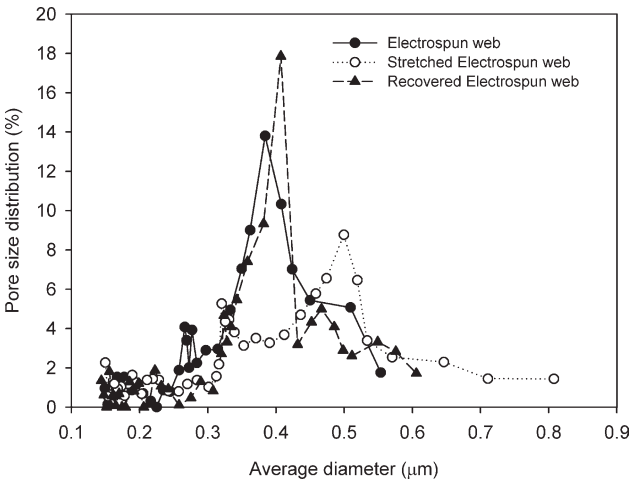

Figure 10 Distribution of the pore diameter for the ESW and the stretched as well as the recovered ESW (thickness: 40 μm).

to the phase change of SMPU, which causes density changes inside the membranes due to the micro-Brownian motion in the soft segment.[29]

Resistance to water penetration

The resistance to water penetration was investigated and the results are shown in Figure 13. The film showed a better resistance to water penetration than the ESW did. The resistance values of the stretched ESW and film decreased a little, but the resistance values of the recovered specimens improved again.

The ESW had an excellent elasticity. Because of these characteristics, as the water pressure increased causing the pore size of the ESW to increase due to stretching, it became easier for water to penetrate. Thus, if a material is manufactured with a base fabric supporting the ESW, it would be expected to show an improved resistance to water penetration.

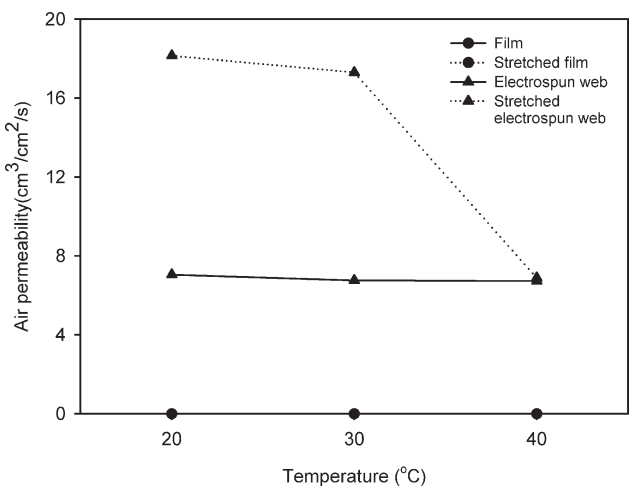

Figure 11 Air permeability of the specimens at various temperatures.

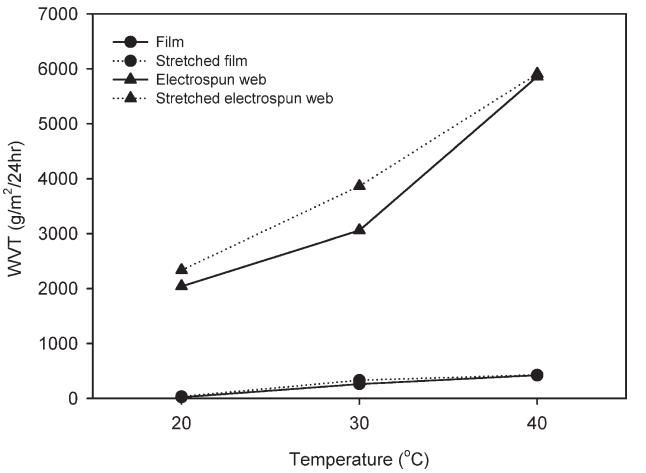

Figure 12 Water vapor transmission of the specimens at various temperatures.

CONCLUSIONS

In this study, the ESW was prepared to develop a protective and thermally intelligent membrane and was compared with the film. Polyurethane with a higher soft segment content was observed to have a higher melting temperature and more crystallinity in the soft segment regions. On the other hand, polyurethane with a higher hard segment content showed an excellent shape recovery and a remarkably higher stress value.

It was observed that the T_{trans} and the heat of fusion of the ESW were much higher than those seen in the film. In addition, the shape recovery of the ESW was improved when compared with the film. The porous structure of the ESW caused a high air permeability and WVT and accordingly, the stretched ESW exhibited enhanced permeabilities below T_{trans}. Therefore, it is concluded that the ESW made of SMPU having a porous structure has a

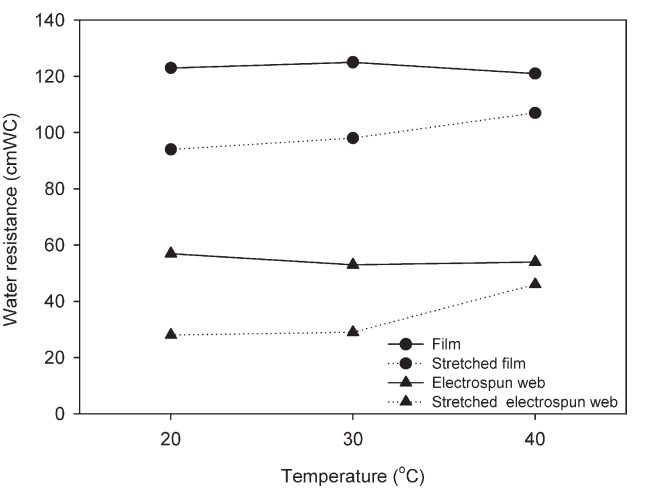

Figure 13 Water resistant values of the specimens at various temperatures.

greater advantage in its shape memory behavior and was found to have a possibility of a protective and thermally intelligent textiles if used under optimum conditions.

References

1. Mattila, H. Intelligent Textile and Clothing; Woolhead Publishing Limited: Cambridge, 2006, p 95.
2. Schmidt, A. Macromol Rapid Commun 2006, 27, 1168.
3. Lendlein, A.; Jiang, H.; Junger, O.; Langer, R. Nature 2005, 434, 879.
4. Scott, T.; Schneider, A.; Cook, W.; Bowman, C. Science 2005, 308, 1615.
5. Behl, M.; Lendlein, A. Mater Today 2007, 10, 20.
6. Liu, C.; Qin, H.; Mather, P. T. J Mater Chem 2007, 17, 1543.
7. Aneja, A.; Wilkes, G. L. Polymer 2002, 43, 5551.
8. Liang, C.; Rogers, C. A.; Malafeew, E. J Intell Mater Syst Struct 1997, 8, 380.
9. Lendlein, A.; Kelch, S. Angew Chem Int Ed Engl 2002, 41 2034.
10. Fu, Y.; Du, H.; Huang, W.; Zhang, S.; Hu, M. Sens Actuators A 2004, 112, 395.
11. Meng, Q.; Hu, J.; Mondal, S. J Membr Sci 2008, 319, 102.
12. Ding, X.; Hu, J.; Tao, X. J Appl Polym Sci 2008, 107, 4061.
13. Chen, Y.; Liu, Y.; Fan, H. J Membr Sci 2007, 287, 192.
14. Mondal, S.; Hu, J. Des Monom Polym 2006, 9, 527.
15. Frenot, A.; Chronakis, I. S. Curr Opin Colloid Interface Sci 2003, 8, 64.
16. Cha, D. I.; Kim, H. Y.; Lee, K. H.; Jung, Y. C.; Cho, J. W.; Chun, B. C. J Appl Polym Sci 2005, 96, 460.
17. Kang, Y. K.; Park, C. H.; Kim, J.; Kang, T. J. Fiber Polym 2007, 8, 564.
18. Lee, B. S.; Chun, B. C.; Chung, Y. C.; Sul, K. I.; Cho, J. W. Macromolecules 2001, 34, 6431.
19. Wang, C. B.; Cooper, S. L. Macromolecules 1983, 16, 775.
20. Cho, J. W.; Lee, S. H. Eur Polym J 2004, 40, 1343.
21. Seymour, R. W.; Ester, G. M.; Cooper, S. L. Macromolecules 1970, 3, 579.
22. Chen, T. K.; Tien, Y. I.; Wei, K. H. Polymer 2000, 41, 1345.
23. Merline, J. J Appl Polym Sci 2008, 107, 4082.
24. Kim, B. K.; Lee, S. Y.; Xu, M. Polymer 1996, 37, 5781.
25. Li, F. K.; Zhang, X.; Hou, J. N.; Xu, M.; Lu, X. L.; Ma, D. Z.; Kim, B. K. J Appl Polym Sci 1997, 64, 1511.
26. Li, F. K.; Hou, J. N.; Zhu, W.; Zhang, X.; Xu, M.; Luo, X. L.; Ma, D. Z.; Kim, B. K. J Appl Polym Sci 1996, 62, 631.
27. Ratna, D.; Karger-Kocsis, J. J Mater Sci 2008, 43, 254.
28. Kaursoin, J.; Agrawal, A. K. J Appl Polym Sci 2007, 103, 2172.
29. Lin, C. Y.; Liao, K. H.; Su, C. F.; Kuo, C. H.; Hsieh, K. H. J Membr Sci 2007, 299, 91.